

Image Captioning via Compact Bidirectional Architecture

Zijie Song*, Yuanen Zhou*[†], Zhenzhen Hu[†], *Member, IEEE*, Daqing Liu, Huixia Ben, Richang Hong, *Member, IEEE*, Meng Wang, *Fellow, IEEE*

Abstract—Most current image captioning models typically generate captions from left-to-right. This unidirectional property makes them can only leverage past context but not future context. Though refinement-based models can exploit both past and future context by generating a new caption in the second stage based on pre-retrieved or pre-generated captions in the first stage, the decoder of these models generally consists of two networks (i.e. a retriever or captioner in the first stage and a captioner in the second stage), which can only be executed sequentially. In this paper, we introduce a Compact Bidirectional Transformer model for image captioning that can leverage bidirectional context implicitly and explicitly while the decoder can be executed parallelly. Specifically, it is implemented by tightly coupling left-to-right(L2R) and right-to-left(R2L) flows into a single compact model to serve as a regularization for implicitly exploiting bidirectional context and optionally allowing explicit interaction of the bidirectional flows, while the final caption is chosen from either L2R or R2L flow in a sentence-level ensemble manner. We conduct extensive ablation studies on MSCOCO benchmark and find that the compact bidirectional architecture and the sentence-level ensemble play more important roles than the explicit interaction mechanism. By combining with word-level ensemble seamlessly, the effect of sentence-level ensemble is further enlarged. We further extend the conventional one-flow self-critical training to the two-flows version under this architecture and achieve new state-of-the-art results in comparison with non-vision-language-pretraining models. Finally, we verify the generality of this compact bidirectional architecture by extending it to LSTM backbone. Source code is available at <https://github.com/YuanEzhou/cbtic>.

Index Terms—Image Captioning, Compact Bidirectional Architecture, Transformer, LSTM.

I. INTRODUCTION

Image captioning [1]–[13], which aims at describing the visual content of an image with natural language sentences, is one of the important tasks to connect vision and language. Inspired by the sequence-to-sequence model [14] for neural machine translation, most proposed models typically follow the encoder/decoder paradigm. In between, a convolutional neural network (CNN) or Transformer is utilized to encode an input image and recurrent neural network (RNN) or Transformer [15] is adopted as sentence decoder to generate a caption.

* denoted equal contribution. [†] denoted the corresponding authors.

Zijie Song is with the School of Big Data and Statistics, Anhui University, Hefei, 230601, China (e-mail: zjsongfut@gmail.com).

Yuanen Zhou is with the Institute of Artificial Intelligence, Hefei Comprehensive National Science Center, and Intelligent Interconnected Systems Laboratory of Anhui Province (Hefei University of Technology), Hefei, 230088 and 230601, China (e-mail: y.e.zhou.hb@gmail.com).

Zhenzhen Hu, Huixia Ben, Richang Hong and Meng Wang are with the School of Computer Science and Information Engineering, Hefei University of Technology, Hefei, 230601, China, (e-mail: huzhen.ice@gmail.com; huixiaben@mail.hfut.edu.cn; hongrc.hfut@gmail.com; eric.mengwang@gmail.com).

Daqing Liu is with JD Explore Academy, JD.com Inc, Beijing, 100176, China, (e-mail: liudq.ustc@gmail.com).

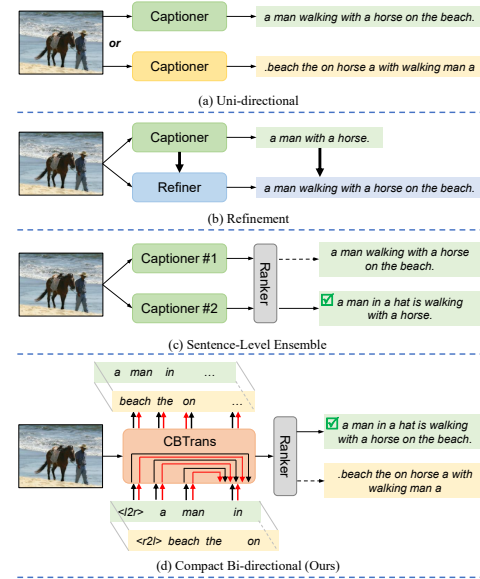


Fig. 1. A conceptual overview of (a) Uni-directional generation, including left-to-right(L2R) and right-to-left(R2L), (b) Refinement-based generation, (c) Sentence-Level Ensemble and (d) our proposed Compact Bidirectional Transformer for Image Captioning (CBTrans), which combines the advantage of (abc), where L2R and R2L ‘flows’ share an unified network and interaction between the two ‘flows’ is optionally allowed inside.

Most current image captioning models [3], [16], [17] typically adopt the uni-directional generation manner (as shown in Fig. 1(a)), which is straightforward. During training and testing, they can only access the past context for the current prediction. This unidirectional property can't make them exploit bidirectional context for better decoding.

To make use of bidirectional context during decoding, refinement-based methods [18]–[22] are proposed recently. The decoder of this type of model typically consists of two networks (as shown in Fig. 1(b)). The first network is usually a primary captioner or an image-text retriever, which is used to generate or retrieve a related sentence. After that, a senior refiner, which is the second network, generates the final caption by being allowed to attend to the sentence produced before. This semantic attention can help the senior refiner to look at both past and future semantic context and thus improve decoding at every time step. However, the two networks in the decoder can only be executed sequentially, which can not make full use of the parallelizability of GPU device.

In this work, we introduce a Compact Bidirectional Transformer model for image captioning (dubbed as CBTrans) that can leverage bidirectional context implicitly and explicitly while the decoder can be executed parallelly. Specifically, it is implemented by tightly coupling the L2R and the R2L flows into a single compact model and optionally allowing explicit

interaction between the two flows (as shown in Fig. 1(d)). The parallelism of our decoder is obvious since it is composed of a single Transformer decoder. We claim our decoder can exploit bidirectional context explicitly since we optionally allow interaction between L2R and R2L flows and implicitly since one copy of shared parameters has the ability of supporting both L2R and R2L decoding. Let's take Fig. 1(d) as an example. During training, each image is associated with two captions instead of single caption as in the conventional L2R captioning models. One caption is from left to right with a $\langle l2r \rangle$ prefix and the other one is from right to left with a $\langle r2l \rangle$ prefix. Inside the CBTrans model, the generation of a target word (e.g., 'walking') can not only depend on previous words in its own flow (e.g., 'a man in a hat is', i.e., past context) but also optionally previous words in the other flow (e.g., 'beach the on horse a with', i.e., future context). The joint loss is composed of both L2R and R2L losses and the model is end-to-end trainable. During inference, CBTrans model takes both $\langle l2r \rangle$ and $\langle r2l \rangle$ as the text input in the first step and optionally allows interaction between the two flows along the entire decoding process. Finally, the output caption of L2R 'flow' and the one of R2L 'flow' are ranked based on their probabilities and the larger one is chosen as the output (i.e. sentence-level ensemble).

We conduct extensive ablation studies on the MSCOCO benchmark dataset to better understand and verify the effectiveness of this model. We find that the **compact** architecture serves as a good regularization for **implicitly** exploiting bidirectional context and a single CBTrans model achieves an effect of **sentence-level ensemble**, which usually needs to train and save two models for improving final predictions as shown in Fig. 1(c). By combining with word-level ensemble, the effect of sentence-level ensemble is further enlarged. Overall, the compact bidirectional architecture and sentence-level ensemble play more important roles than the **explicit** interaction mechanism. We further extend the conventional one-flow self-critical training to the two-flows version under this model architecture and achieve new state-of-the-art results in comparison with non-vision-language-pretraining models. Finally, we verify the generality of this compact bidirectional architecture by extending it to LSTM backbone and proposing the CBLSTM model.

The main contributions are summarized as follows:

- We introduce a Compact Bidirectional Transformer model for image captioning that can leverage bidirectional context implicitly and explicitly while the decoder is parameter-efficient and can be executed parallelly. And we conduct extensive ablation studies to better understand this architecture.
- We further propose to combine word-level and sentence-level ensemble seamlessly and extend the conventional one-flow self-critical training to the two-flows version under this architecture and achieve new state-of-the-art results in comparison with non-vision-language-pretraining models.
- Finally, we verify the generality of this compact bidirectional architecture by extending it to LSTM backbone and proposing the CBLSTM model.

The remainder of this paper is organized as follows. Section II reviews related works. Section III elaborates on the proposed approach. The analysis and discussion of the experimental results are presented in Section IV. Finally, we conclude our work in Section V.

II. RELATED WORK

A. Image Captioning

Over the last few years, a broad collection of methods have been proposed in the field of image captioning. In a nutshell, we have gone through grid-feature [23], [24] then region-feature [25] and relation-aware visual feature [2], [26] on the image encoding side. On the sentence decoding side, we have witnessed LSTM [1], CNN [27] and Transformer [28] equipped with various attention [3], [29], [30] as the decoder. On the training side, models are typically trained by cross-entropy loss and then Reinforcement Learning [31], which enables the use of non-differentiable caption metrics as optimization objectives and makes a notable achievement. Recently, vision-language pre-training has also been adopted for image captioning and shows remarkable results. These models [32]–[34] are firstly pre-trained on large image-text corpus and then finetuned. Though impressive performance has been achieved, most state-of-the-art models adopt the left-to-right generation manner, which is straightforward but can't exploit bidirectional context. To make use of bidirectional context as far as possible, refinement-based methods are proposed recently, where [18], [19], [21] generate a primary caption and [20], [22] retrieve a related primary caption in the first stage and both them generate a senior caption in the second stage based on the primary caption. There is also an early work [35] that tries to overcome the shortcomings of unidirectional model by combining the output captions of two separate forward and backward LSTM networks. Different from these models, CBTrans is a single Compact Bidirectional Transformer model and CBLSTM is a single Compact Bidirectional LSTM model.

B. Multi-task Learning

Multi-task learning is a useful learning paradigm to improve the supervision and the generalization performance of a task by jointly training it with related tasks [36]. Here, we only review some multi-task learning works related to captioning. To the best of our knowledge, there are roughly two types so far. One is to jointly train the task of captioning and syntax generation (e.g. Part-of-Speech) [37]–[40]. The other one is to train a unified captioning model on multilingual (e.g. English and Chinese) captioning datasets [41]–[44]. Different from the above multi-task learning methods, one task is the L2R generation and the other one is the R2L generation in our method.

C. Neural Machine Translation

Neural Machine Translation (NMT) has an important impact on the research of captioning task. The standard encoder-decoder paradigm is derived from NMT [14], [45]. A complete review is beyond the scope of this paper and we only focus on works related to endow decoder with bidirectional ability. [46] trained a backward decoder jointly with a forward

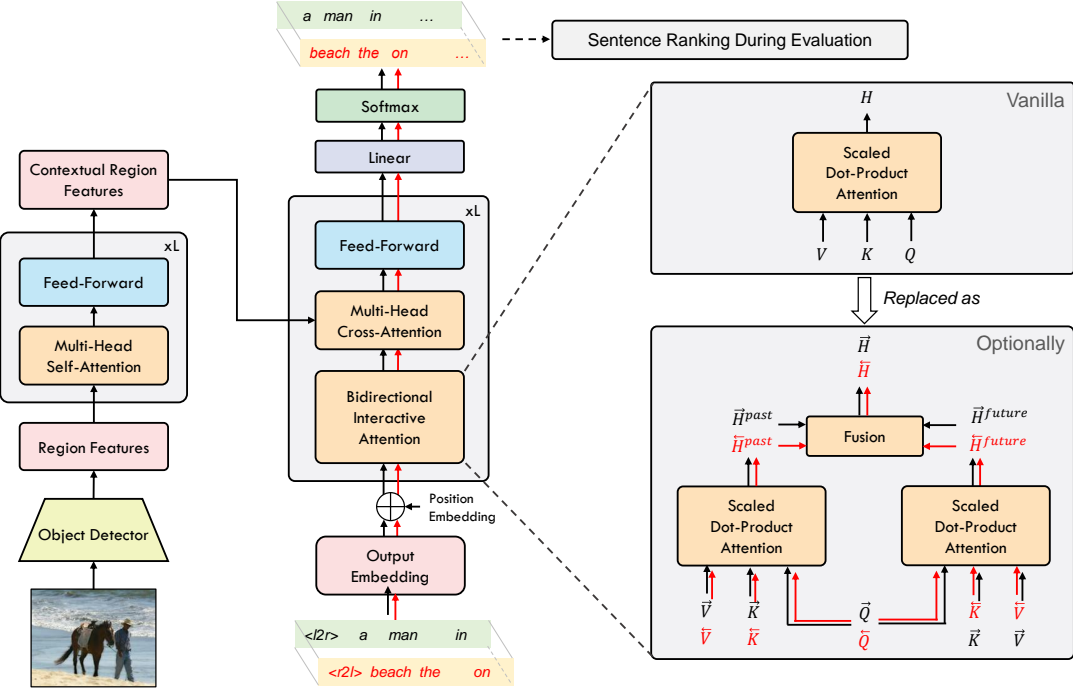


Fig. 2. Illustration of Compact Bidirectional Transformer for Image Captioning (CBTrans). CBTrans model composes of an encoder (in the left) and a decoder (in the middle). An intuitional illustration of the extension of the standard Scaled Dot-Product Attention module is shown on the right. Notice that the Residual Connections, Layer Normalization are omitted. The subscript of head i in $Q/K/V/H$ is omitted for brevity. Right-to-right (R2L) flow is marked in red. Best view in color.

decoder by matching their output probabilities to iteratively improve each other. [47] proposed to further encourage conventional auto-regressive decoder to plan ahead by distilling bidirectional knowledge learned in BERT [48]. [49] proposed asynchronous bidirectional decoding for NMT by equipping the conventional attentional forward decoder with an auxiliary backward decoder. [50] proposed a synchronous bidirectional neural machine translation that predicts its outputs using left-to-right and right-to-left decoding simultaneously and interactively. This work pursues the spirit of [50] for image captioning and we find that it is the compact bidirectional architecture and sentence-level ensemble mechanism instead of explicit interaction that contributes more to the model. This is overlooked in [50] and indicates that explicit interaction is overestimated. What's more, we further propose to combine word-level and sentence-level ensemble seamlessly and extend the conventional one-flow self-critical training to the two-flows version.

III. APPROACH

In this section, we first present two representative compact bidirectional architectures built on the well-known Transformer [15] and LSTM [51] and then introduce the training procedure for model optimization.

A. CBTrans Model

Firstly, a pre-trained object detector [52] represents an image I as a set of region features. Then given the image region features, CBTrans aims to take advantage of bidirectional property in a single model to generate a sensible caption. The architecture of CBTrans model is illustrated in Fig. 2, which consists of an encoder and decoder.

1) Image Features Encoder.: The encoder, which is basically the same as the Transformer encoder [15], takes the image region features as inputs and outputs the contextual region features. It consists of a stack of L identical layers. Each layer has two sublayers. The first is a multi-head self-attention sublayer and the second is a position-wise feed-forward sublayer. Both sublayers are followed by residual connection [53] and layer normalization [54] operations for stable training. Multi-head self-attention builds on the scaled dot-product attention, which operates on a query Q , key K and value V as:

$$\text{Attention}(Q, K, V) = \text{softmax}\left(\frac{QK^T}{\sqrt{d_k}}\right)V, \quad (1)$$

where d_k is the dimension of the key. Multi-head self-attention firstly projects the queries, keys and values h times with different learned linear projections and then computes scaled dot-product attention for each one. After that, it concatenates the results and projects them with another learned linear projection:

$$H_i = \text{Attention}(QW_i^Q, KW_i^K, VW_i^V), \quad (2)$$

$$\text{MultiHead}(Q, K, V) = \text{Concat}(H_1, \dots, H_h)W^O, \quad (3)$$

where $W_i^Q, W_i^K \in \mathbb{R}^{d_{\text{model}} \times d_k}$, $W_i^V \in \mathbb{R}^{d_{\text{model}} \times d_v}$ and $W^O \in \mathbb{R}^{hd_v \times d_{\text{model}}}$. The self-attention in the encoder performs attention over itself, i.e., $(Q = K = V)$, which is the image region features in the first layer. After a multi-head self-attention sublayer, the position-wise feed-forward sublayer (FFN) is applied to each position separately and identically:

$$\text{FFN}(x) = \max(0, xW_1 + b_1)W_2 + b_2, \quad (4)$$

where $W_1 \in \mathbb{R}^{d_{model} \times d_{ff}}$, $W_2 \in \mathbb{R}^{d_{ff} \times d_{model}}$, $b_1 \in \mathbb{R}^{d_{ff}}$ and $b_2 \in \mathbb{R}^{d_{model}}$ are learnable parameter matrices.

2) *Captioning Decoder*: The decoder takes contextual region features and a pair of L2R and R2L word sequences of each image as input and outputs a pair of predicted words probability sequences. To make use of order information, position encodings [15] are added to word embedding features. It is worth emphasizing that the L2R and R2L flows in the decoder run in parallel and the explicit bidirectional interaction only optionally happens in the mask multi-head bidirectional interactive attention sublayer. Specifically, the decoder consists of L identical layers and each layer has three sublayers: a masked multi-head bidirectional interactive attention sublayer, a multi-head cross-attention sublayer and a position-wise feed-forward sublayer. Residual connection and layer normalization are also applied after each sublayer. The multi-head cross-attention is similar to the multi-head self-attention mentioned above except that the key and value are now contextual region features and the query is the output of its previous sublayer. The masked multi-head bidirectional interactive attention sublayer can be seen as an optional extension of the masked multi-head attention sublayer in the original Transformer decoder [15]. The main difference between them lies in the scaled dot-product attention module. An intuitionial illustration is shown in the right of Fig. 2. Formally, the scaled dot-product attention for each head i in the original masked multi-head attention module is extended to:

$$\begin{aligned}\vec{H}_i^{past} &= \text{Attention}(\vec{Q}_i, \vec{K}_i, \vec{V}_i) \\ \vec{H}_i^{future} &= \text{Attention}(\vec{Q}_i, \vec{K}_i, \vec{V}_i), \\ \vec{H}_i &= \vec{H}_i^{past} + \lambda * \text{AF}(\vec{H}_i^{future})\end{aligned}\quad (5)$$

where \vec{H}_i^{past} is the conventional one to capture past context and \vec{H}_i^{future} is the extended part to capture future context by using query in the L2R direction and key/value in R2L direction. \vec{H}_i is the bidirectional-aware state of L2R direction by non-linearly fusing past and future context and AF denotes activation function, such as Relu or Tanh. It is worth noting that the self-attention in the decoder usually is equipped with a lower triangular matrix mask for preventing positions from attending to subsequent positions and we omit it here for brevity. And the bidirectional-aware state of backward direction \vec{H}_i can be symmetrically computed as:

$$\vec{H}_i = \text{Attention}(\vec{Q}_i, \vec{K}_i, \vec{V}_i) + \lambda * \text{AF}(\text{Attention}(\vec{Q}_i, \vec{K}_i, \vec{V}_i)). \quad (6)$$

In particular, the masked multi-head bidirectional interactive attention sublayer degrades to the original masked multi-head attention sublayer when $\lambda = 0$.

Finally, we use a learned linear transformation and softmax function to convert the decoder output to a pair of predicted next-token probabilities $p(\vec{y}_t | \vec{y}_{<t}, \vec{y}_{<t}, I; \theta)$ and $p(\vec{y}_t | \vec{y}_{<t}, \vec{y}_{<t}, I; \theta)$, where $\vec{y}_{<t}$ ($\vec{y}_{<t}$) denotes the words sequence of L2R (R2L) direction before the t -th word of target \vec{y} (\vec{y}) and θ is the shared parameters.

B. CBLSTM Model

For LSTM [51] backbone, we adopt the popular Up-Down [25] model as our start point and our final compact

bidirectional LSTM model (dubbed as CBLSTM) is illustrated in Fig. 3, which also consists of an encoder and a decoder.

1) *Image Features Encoder*: The encoder is just a vanilla object detector [52] and followed by a feature projection matrix, which represents an image I as a set of region features $V = \{v_i\}_{i=1}^R$.

2) *Captioning Decoder*: The decoder is mainly composed of two LSTM layers where the first one is the Attention LSTM and the second one is the Language LSTM. Each layer is indicated with the corresponding subscript in the following equations. Instead of having only one L2R 'flow' as in conventional Up-Down decoder [25], the decoder of our CBLSTM model processes both L2R and R2L flows simultaneously. The L2R flow has a $\langle l2r \rangle$ prefix and the R2L one has a $\langle r2l \rangle$ prefix. Specifically, at time step t , the Attention LSTM takes previous hidden state outputs of the Language LSTM on both flows (i.e., \vec{h}_{t-1}^2 and \vec{h}_{t-1}^1), previous word embedding of both flows (i.e., $\vec{e}_{t-1} = W_e \vec{y}_{t-1}$ and $\vec{e}_{t-1} = W_e \vec{y}_{t-1}$) and mean-pooled image feature $\vec{v} = \frac{1}{R} \sum_i v_i$ as input and outputs hidden state of both flows:

$$\begin{aligned}\vec{h}_t^1 &= \text{LSTM}_1([\vec{h}_{t-1}^2; \vec{v}; \vec{e}_{t-1}], \vec{h}_{t-1}^1) \\ \vec{h}_t^1 &= \text{LSTM}_1([\vec{h}_{t-1}^2; \vec{v}; \vec{e}_{t-1}], \vec{h}_{t-1}^1),\end{aligned}\quad (7)$$

where $[;]$ denotes concatenation, W_e is the word embedding matrix and \vec{y}_{t-1} (\vec{y}_{t-1}) is the word of L2R (R2L) flow at time step $t-1$. Given \vec{h}_t^1 , the attended image feature of L2R flow is calculated as:

$$\begin{aligned}\vec{z}_{i,t} &= w_a^T \tanh(W_{va} v_i + W_{ha} \vec{h}_t^1) \\ \vec{\beta}_t &= \text{softmax}(z_t), \quad \vec{v}_t = \sum_{i=1}^R \vec{\beta}_{i,t} v_i,\end{aligned}\quad (8)$$

where w_a , W_{va} and W_{ha} are learned weights. And \vec{v}_t can be calculated in the same way. Then the Language LSTM takes the attended image features (i.e., \vec{v}_t and \vec{v}_t) and hidden state of Attention LSTM (i.e., \vec{h}_t^1 and \vec{h}_t^1) as input and outputs the language hidden states of both flows as:

$$\begin{aligned}\vec{h}_t^2 &= \text{LSTM}_2([\vec{h}_t^1; \vec{v}_t], \vec{h}_{t-1}^2) \\ \vec{h}_t^2 &= \text{LSTM}_2([\vec{h}_t^1; \vec{v}_t], \vec{h}_{t-1}^2).\end{aligned}\quad (9)$$

Optionally, the language hidden states can be further fed into a Bidirectional Interaction Module to obtain bidirectional context as:

$$\begin{aligned}\vec{h}_t^2 &= \vec{h}_t^2 + \lambda * \text{AF}(\vec{h}_t^2) \\ \vec{h}_t^2 &= \vec{h}_t^2 + \lambda * \text{AF}(\vec{h}_t^2),\end{aligned}\quad (10)$$

where AF denotes activation function and λ is the weight balance.

Finally, the language hidden states are converted to conditional probability distribution over possible output words as:

$$\begin{aligned}p(\vec{y}_t | \vec{y}_{<t}, \vec{y}_{<t}, I; \theta) &= \text{softmax}(W_o \vec{h}_t^2 + b_o) \\ p(\vec{y}_t | \vec{y}_{<t}, \vec{y}_{<t}, I; \theta) &= \text{softmax}(W_o \vec{h}_t^2 + b_o),\end{aligned}\quad (11)$$

where W_o and b_o are learned weights and biases, $\vec{y}_{<t}$ ($\vec{y}_{<t}$) denotes the words sequence of L2R (R2L) direction before the t -th word and θ is the shared parameters.

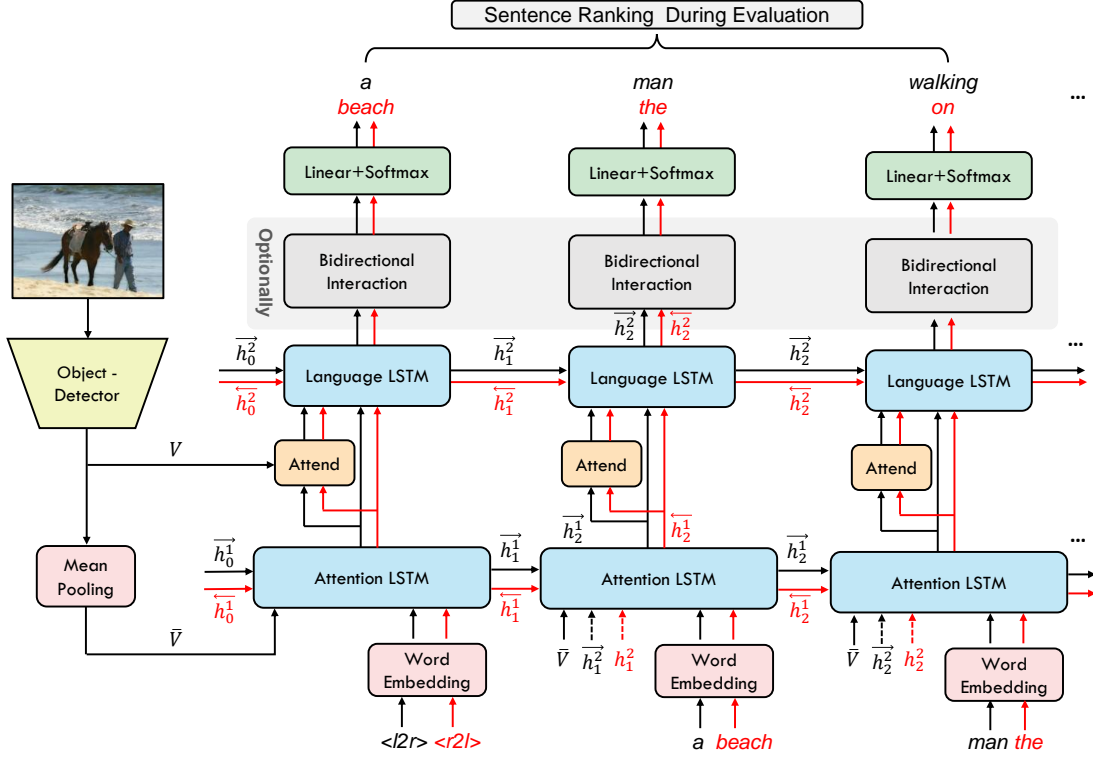


Fig. 3. Illustration of Compact Bidirectional LSTM model (CBLSTM) for Image Captioning. Best view in color.

C. Training

The whole training procedure of both models includes two stages. At the first training stage, given a triple (I, \vec{y}, \vec{y}) , we pad the two sentences to equal length T without loss of generality, i.e., $\vec{y} = (\vec{y}_1, \vec{y}_2, \dots, \vec{y}_T)$ and $\vec{y} = (\vec{y}_1, \vec{y}_2, \dots, \vec{y}_T)$. We optimize the model by minimizing joint cross-entropy (XE) loss, which is composed of a L2R and R2L XE loss:

$$L_{XE}(\theta) = - \sum_{t=1}^T \{ \log p(\vec{y}_t | \vec{y}_{<t}, \vec{y}_{<t}, I; \theta) + \log p(\vec{y}_t | \vec{y}_{<t}, \vec{y}_{<t}, I; \theta) \}. \quad (12)$$

In order to prevent the bidirectional model from learning to directly generate the second half of L2R flow by copying the first half of R2L flow and vice versa, \vec{y} is chosen from the rest caption annotations of the same image (each image is annotated with five captions in the dataset) then reversed and paired with \vec{y} .

At the second training stage, we jointly finetune the model using self-critical training (SC) [31] for both L2R and R2L directions and the gradient can be expressed as:

$$\nabla_{\theta} L_{SC}(\theta) = -\frac{1}{N} \sum_{n=1}^N \{ (R(\vec{y}^n) - \vec{b}) \nabla_{\theta} \log p(\vec{y}^n | I; \theta) + (R(\vec{y}^n) - \vec{b}) \nabla_{\theta} \log p(\vec{y}^n | I; \theta) \}, \quad (13)$$

where R is the CIDEr [55] score function, and b is the baseline score. We adopt the baseline score proposed in [56], where the baseline score is defined as the average reward of the rest samples rather than the original greedy decoding reward. We

sample $N = 5$ captions for each image and each direction and \vec{y}^n (\vec{y}^n) is the n -th sampled caption of L2R (R2L) direction.

IV. EXPERIMENTS

A. Dataset and Evaluation Metrics.

MSCOCO [66] is the widely used benchmark for image captioning. We use the 'Karpathy' splits [67] for offline experiments. This split contains 113,287 training images, 5,000 validation images and 5,000 testing images. Each image has 5 captions. We also upload generated captions of MSCOCO official testing set, which contains 40,775 images for online evaluation. The quality of captions is evaluated by standard metrics [66], including BLEU-1/4 [68], METEOR [69], ROUGE [70], SPICE [71], and CIDEr [55], denoted as B1/4, M, R, S, and C for short.

B. Implementation Details.

Each image is represented as a set of region features with 2,048 dimensions extracted by object detector [52]. We try two kinds of features, i.e., Up-Down feature with 36 regions per image [25], and VinVL feature with up to 50 regions per image [34], which is extracted by a more powerful detector. The dictionary is built by dropping the words that occur less than 5 times and ends up with a vocabulary of 9,487. Captions longer than 16 words are truncated. Our CBTrans model almost follows the same model hyper-parameters setting as in [15] ($d_{model} = 512, d_k = d_v = 64, d_{ff} = 2048, L = 6, h = 8, p_{dropout} = 0.1$). And the word embedding size, LSTM hidden state size and image feature projection size of our CBLSTM model are all set to 1,024. As for the

TABLE I

PERFORMANCE COMPARISONS ON MSCOCO KARPATHY TEST SPLIT, WHERE B@N, M, R, C AND S ARE SHORT FOR BLEU@N, METEOR, ROUGE-L, CIDEr AND SPiCE SCORES. ALL VALUES ARE REPORTED AS PERCENTAGE (%). Σ INDICATES MODEL ENSEMBLE.

	Cross-Entropy Loss								CIDEr Score Optimization							
	B@1	B@2	B@3	B@4	M	R	C	S	B@1	B@2	B@3	B@4	M	R	C	S
LSTM [1]	-	-	-	29.6	25.2	52.6	94.0	-	-	-	-	31.9	25.5	54.3	106.3	-
SCST [31]	-	-	-	30.0	25.9	53.4	99.4	-	-	-	-	34.2	26.7	55.7	114.0	-
LSTM-A [57]	75.4	-	-	35.2	26.9	55.8	108.8	20.0	78.6	-	-	35.5	27.3	56.8	118.3	20.8
RFNet [58]	76.4	60.4	46.6	35.8	27.4	56.5	112.5	20.5	79.1	63.1	48.4	36.5	27.7	57.3	121.9	21.2
Up-Down [25]	77.2	-	-	36.2	27.0	56.4	113.5	20.3	79.8	-	-	36.3	27.7	56.9	120.1	21.4
GCN-LSTM [26]	77.3	-	-	36.8	27.9	57.0	116.3	20.9	80.5	-	-	38.2	28.5	58.3	127.6	22.0
LBPF [59]	77.8	-	-	37.4	28.1	57.5	116.4	21.2	80.5	-	-	38.3	28.5	58.4	127.6	22.0
SGAE [2]	77.6	-	-	36.9	27.7	57.2	116.7	20.9	80.8	-	-	38.4	28.4	58.6	127.8	22.1
AoANet [29]	77.4	-	-	37.2	28.4	57.5	119.8	21.3	80.2	-	-	38.9	29.2	58.8	129.8	22.4
X-LAN [3]	78.0	62.3	48.9	38.2	28.8	58.0	122.0	21.9	80.8	65.6	51.4	39.5	29.5	59.2	132.0	23.4
M^2 [28]	-	-	-	-	-	-	-	-	80.8	-	-	39.1	29.2	58.6	131.2	22.6
X-Transformer [3]	77.3	61.5	47.8	37.0	28.7	57.5	120.0	21.8	80.9	65.8	51.5	39.7	29.5	59.1	132.8	23.4
RSTNet [16]	-	-	-	-	-	-	-	-	81.8	-	-	40.1	29.8	59.5	135.6	23.3
SGT [60]	78.0	-	-	38.0	28.8	58.1	120.8	-	81.4	-	-	39.8	29.6	59.2	132.9	-
MD-SAN [61]	-	-	-	-	-	-	-	-	81.5	-	-	39.8	29.6	59.1	135.1	23.2
FeiM [62]	78.6	-	-	38.1	28.8	58.3	122.5	21.8	81.9	-	-	40.5	29.9	59.8	135.2	23.7
ACFiC [63]	77.8	62.2	48.4	37.6	28.6	58.7	122.7	21.9	81.3	66.6	52.4	39.6	29.4	59.4	134.2	23.3
I^2 OA [64]	76.5	-	-	36.9	28.9	57.8	121.3	22.1	81.9	-	-	40.5	29.9	59.6	136.2	23.5
CBLSTM	77.6	62.0	48.3	37.5	28.9	57.9	121.0	22.0	80.7	65.3	50.4	38.1	29.0	58.2	133.6	22.8
CBTrans	78.0	62.2	48.5	37.5	29.1	58.2	122.6	22.3	81.4	66.5	51.9	39.6	29.9	59.1	136.9	24.0
Ensemble																
SCST [31] Σ	-	-	-	32.8	26.7	55.1	106.5	-	-	-	-	35.4	27.1	56.6	117.5	-
RFNet [58] Σ	77.4	61.6	47.9	37.0	27.9	57.3	116.3	20.8	80.4	64.7	50.0	37.9	28.3	58.3	125.7	21.7
GCN-LSTM [26] Σ	77.4	-	-	37.1	28.1	57.2	117.1	21.1	80.9	-	-	38.3	28.6	58.5	128.7	22.1
SGAE [2] Σ	-	-	-	-	-	-	-	-	81.0	-	-	39.0	28.4	58.9	129.1	22.2
HIP [65] Σ	-	-	-	38.0	28.6	57.8	120.3	21.4	-	-	-	39.1	28.9	59.2	130.6	22.3
AoANet [29] Σ	78.7	-	-	38.1	28.5	58.2	122.7	21.7	81.6	-	-	40.2	29.3	59.4	132.0	22.8
M^2 T [28] Σ	-	-	-	-	-	-	-	-	82.0	-	-	40.5	29.7	59.5	134.5	23.5
X-LAN [3] Σ	78.8	63.4	49.9	39.1	29.1	58.5	124.5	22.2	81.6	66.6	52.3	40.3	29.8	59.6	133.7	23.6
X-Transformer [3] Σ	77.8	62.1	48.6	37.7	29.0	58.0	122.1	21.9	81.7	66.8	52.6	40.7	29.9	59.7	135.3	23.8
CBLSTM	78.3	62.8	49.1	38.2	29.2	58.5	123.1	22.2	81.5	66.3	51.5	39.1	29.3	58.8	135.6	23.0
CBTrans	79.1	63.9	50.3	39.4	29.8	59.3	127.8	23.1	82.7	67.9	53.5	41.1	30.4	60.1	140.3	24.3

TABLE II

PERFORMANCE OF CBTRANS ON MSCOCO VALIDATION SET WITH DIFFERENT ACTIVATION FUNCTIONS AND λ . ONLY CROSS-ENTROPY LOSS IS USED AND BEAM SIZE IS SET TO 1.

Metrics \ λ	0.0		0.1		0.4		
	AF	B@1	C	B@1	C	B@1	C
Up-Down Feat.							
Tanh		76.5	114.2	76.5	114.0	76.8	114.4
ReLU		76.5	114.2	76.9	115.0	76.6	114.4
VinVL Feat.							
ReLU		78.1	121.6	78.5	122.4	78.3	121.5

TABLE III

PERFORMANCE OF CBLSTM ON MSCOCO VALIDATION SET WITH DIFFERENT λ . BEAM SIZE IS SET TO 1 AND RELU ACTIVATION FUNCTION IS SELECTED AS DEFAULT.

λ	Cross-Entropy Loss			
	B@4	M	R	C
0.0	37.3	28.7	58.1	120.6
0.1	37.4	28.8	58.1	120.8
0.2	37.6	28.7	58.3	121.4
0.4	37.7	28.9	58.4	121.4

training process, we train CBTrans (CBLSTM) under cross-entropy loss for 15 (30) epochs with a mini batch size of 10 (32). The optimizer in [15] is used with a learning rate initialized by 5e-4 and the warmup step is set to 20,000 for CBTrans model and Adam [72] optimizer is used with learning rate initialized by 5e-4 and decayed by a factor 0.8 every three epochs for CBLSTM model. We increase

the scheduled sampling probability by 0.05 every 5 epochs. We then optimize the CIDEr score with self-critical training for another 15 (20) epochs with an initial learning rate of 1e-5 (5e-5) for CBTrans (CBLSTM) model. During testing, unless stated otherwise, we use the standard beam search for conventional Transformer and Up-Down models with beam size 3, which is the best width based on our observation. It is worth noting that the beam search method for CBTrans and CBLSTM models is a little different from the standard one. Specifically, if the total beam size is 4, then both L2R and R2L flows should independently keep a standard beam search with beam size 2 for each step. Unless stated otherwise, the beam size of each flow is set to 2 for CBTrans and CBLSTM models.

C. Quantitative Results

In this section, we will quantitatively analyze our models in detail by answering the following questions.

1) *What is the effect of Fusion function with different λ ?*: Following previous practice [50], we choose to use the simple non-linear fusion mechanism. From Table II, we can find that the explicit interaction mechanism only improves slightly over the baseline ($\lambda = 0$) when proper $\lambda = 0.1$ is selected. This indicates that the explicit interaction mechanism is not the main contributor of this model, which is different from [50], and motivates us to further decipher this architecture. In the following, we select ReLU and set $\lambda = 0.1$ for CBTrans model as default, unless stated otherwise. We also observe

TABLE IV

ABLATION STUDIES OF CBTRANS MODEL ON MSCOCO VALIDATION SET. THE DEFAULT RANDOM SEED IS 0.

Models	Metrics	Cross-Entropy Loss			
		B@4	M	R	C
Up-Down Feat.					
1	Transformer(L2R)	35.4	27.8	56.3	111.7
2	Transformer(L2R-seed1)	35.4	27.7	56.3	112.3
3	Sentence-Level Ensemble	35.1	28.1	56.4	112.5
4	Transformer(L2R)	35.4	27.8	56.3	111.7
5	Transformer(R2L)	33.9	27.1	55.2	109.6
6	Sentence-Level Ensemble	34.6	27.8	56.0	111.7
7	CBTrans(only keep R2L during eval.)	34.3	27.5	56.0	112.6
8	CBTrans(only keep L2R during eval.)	35.7	27.7	56.7	113.4
9	CBTrans	35.6	28.1	56.8	114.4
VinVL Feat.					
10	Transformer(L2R)	37.1	28.4	57.3	117.6
11	Transformer(L2R-seed1)	36.6	28.6	57.2	117.3
12	Sentence-Level Ensemble	36.8	28.8	57.4	118.5
13	Transformer(L2R)	37.1	28.4	57.3	117.6
14	Transformer(R2L)	35.5	28.1	56.9	117.0
15	Sentence-Level Ensemble	37.1	29.0	57.9	119.9
16	CBTrans(only keep R2L during eval.)	36.1	28.4	57.3	119.4
17	CBTrans(only keep L2R during eval.)	37.8	28.9	58.0	121.3
18	CBTrans	37.8	29.1	58.2	121.8
19	Transformer(L2R+L2R)	37.1	28.5	57.4	119.0

similar results for CBLSTM model as shown in Table III. As an extreme try, we set $\lambda = 0$ for CBLSTM model in the following, which means we discard the explicit Bidirectional Interaction module.

TABLE V

PERFORMANCE OF CBTRANS MODEL COMBINED WITH MODEL ENSEMBLE ON MSCOCO VALIDATION SET. '2' INDICATES WE AVERAGE THE WORD-LEVEL OUTPUT PROBABILITY DISTRIBUTIONS OF TWO INDEPENDENTLY TRAINED INSTANCES WITH DIFFERENT PARAMETER INITIALIZATION. BEAM SIZE IS SET TO 1 AND VINVL FEATURE IS USED.

Models	Metrics	Cross-Entropy Loss			
		B@4	M	R	C
CBTrans*2		38.3	29.4	58.9	125.3
CBTrans(only keep L2R during eval.)*2		37.4	28.9	58.3	122.5
CBTrans*3		39.2	29.7	59.2	127.4
CBTrans(only keep L2R during eval.)*3		38.3	29.3	58.8	125.1
CBTrans*4		39.1	29.7	59.3	127.6
CBTrans(only keep L2R during eval.)*4		38.6	29.3	59.0	125.5

TABLE VI

PERFORMANCE OF CBLSTM MODEL COMBINED WITH MODEL ENSEMBLE ON MSCOCO VALIDATION SET. '2' INDICATES WE AVERAGE THE WORD-LEVEL OUTPUT PROBABILITY DISTRIBUTIONS OF TWO INDEPENDENTLY TRAINED INSTANCES WITH DIFFERENT PARAMETER INITIALIZATION. BEAM SIZE IS SET TO 1 AND VINVL FEATURE IS USED.

Models	Metrics	Cross-Entropy Loss			
		B@4	M	R	C
CBLSTM*2		37.7	28.9	58.4	121.5
CBLSTM(only keep L2R during eval.)*2		36.5	28.2	57.6	117.3
CBLSTM*3		38.1	29.0	58.7	122.7
CBLSTM(only keep L2R during eval.)*3		36.7	28.3	57.8	117.7
CBLSTM*4		38.4	29.1	58.7	123.3
CBLSTM(only keep L2R during eval.)*4		36.6	28.4	57.8	118.1

2) *What is the effect of each component that constitutes the compact bidirectional architecture?:* To further investigate the effectiveness of our models and each component, we

conduct substantial ablation studies, as shown in Table IV. Before diving into the details, we emphasize that our model doesn't increase any model parameters except two special symbols (i.e., $\langle l2r \rangle$ and $\langle r2l \rangle$) embedding compared to the standard baseline model and they share the same training script.

Firstly, by comparing the 9th row with the 1st and 5th rows, we can find that the whole CBTrans model outperforms Transformer(L2R) and Transformer(R2L) models more than 2.7% in CIDEr metric. And the advantage of our CBTrans model is more obvious when using better VinVL feature by comparing the 18th row with the 10th row (e.g., more than 4.2% gain in CIDEr metric). This proves the overall effectiveness of CBTrans model. We can also see similar performance gains (e.g., about 2.9% gain in CIDEr metric) for CBLSTM model by comparing the 3rd row with the 1st row in Table IX.

Secondly, by comparing the 7th/8th row with the 5th/1st row in Table IV, we can find that the **compact** architecture of CBTrans model can serve as a good regularization by improving the performance from 109.6/111.7 CIDEr to 112.6/113.4 CIDEr. And we can also see similar trend when using better VinVL feature by comparing the 16th/17th row with the 14th/13th row. However, the regularization effect is not obvious as for CBLSTM model. One possible reason is that the model capacity of CBLSTM is very limited compared to CBTrans model.

Thirdly, we investigate the effect of sentence-level ensemble, which is a natural part of our compact bidirectional models since we have to choose one final caption from the output of L2R and R2L 'flow'. By comparing the 9th row with the 8th row of Table IV, we can see the effect of sentence-level ensemble mechanism by improving the METEOR metric from 27.7 to 28.1. The effect of sentence-level ensemble is further enlarged when combined with model ensemble, which typically averages the word-level output probability distributions of multiple independently trained instances with different parameter initialization. From Table V, we can see that sentence-level ensemble contributes more than 2% in CIDEr metric at all model ensemble cases for CBTrans model. As for CBLSTM model, the sentence-level ensemble contributes more than 4% in CIDEr metric at all model ensemble cases, as shown in Table VI.

Additionally, we also experimentally construct other two sentence-level ensemble models during evaluation to check the generality of this mechanism, where one is an ensemble of two Transformer(L2R) models and the other one is an ensemble of Transformer (L2R) and Transformer (R2L) models. By observing the 3rd/6th/12th/15th rows of Table IV, we can find that this mechanism can still bring non-trivial improvement on METEOR metric but at the cost of saving and running two models.

Finally, we also report the performance comparison between our compact bidirectional model and the unidirectional counterpart after CIDEr score optimization. Basically, CBTrans model has a similar advantage as in the first training stage as shown in Table VIII, e.g., improving the conventional Transformer(L2R) model from 127.6 (22.6) to

TABLE VII

LEADERBOARD OF THE PUBLISHED STATE-OF-THE-ART IMAGE CAPTIONING MODELS ON THE MSCOCO ONLINE TESTING SERVER, WHERE B@N, M, R, AND C ARE SHORT FOR BLEU@N, METEOR, ROUGE-L, AND CIDEr SCORES. ALL VALUES ARE REPORTED AS PERCENTAGE (%).

Model	Metrics		BLEU-1		BLEU-2		BLEU-3		BLEU-4		METEOR		ROUGE		CIDEr	
	c5	c40	c5	c40	c5	c40										
SCST [31]	78.1	93.7	61.9	86.0	47.0	75.9	35.2	64.5	27.0	35.5	56.3	70.7	114.7	116.7		
Up-Down [25]	80.2	95.2	64.1	88.8	49.1	79.4	36.9	68.5	27.6	36.7	57.1	72.4	117.9	120.5		
RFNet [58]	80.4	95.0	64.9	89.3	50.1	80.1	38.0	69.2	28.2	37.2	58.2	73.1	122.9	125.1		
GCN-LSTM [26]	80.8	95.9	65.5	89.3	50.8	80.3	38.7	69.7	28.5	37.6	58.5	73.4	125.3	126.5		
SGAE [2]	81.0	95.3	65.6	89.5	50.7	80.4	38.5	69.7	28.2	37.2	58.6	73.6	123.8	126.5		
ETA [73]	81.2	95.0	65.5	89.0	50.9	80.4	38.9	70.2	28.6	38.0	58.6	73.9	122.1	124.4		
AoANet [29]	81.0	95.0	65.8	89.6	51.4	81.3	39.4	71.2	29.1	38.5	58.9	74.5	126.9	129.6		
GCN-LSTM+HIP [65]	81.6	95.9	66.2	90.4	51.5	81.6	39.3	71.0	28.8	38.1	59.0	74.1	127.9	130.2		
M^2 T [28]	81.6	96.0	66.4	90.8	51.8	82.7	39.7	72.8	29.4	39.0	59.2	74.8	129.3	132.1		
X-Transformer [3]	81.9	95.7	66.9	90.5	52.4	82.5	40.3	72.4	29.6	39.2	59.5	75.0	131.1	133.5		
GET [74]	81.6	96.1	66.5	90.9	51.9	82.8	39.7	72.9	29.4	38.8	59.1	74.4	130.3	132.5		
RSTNet [16]	82.1	96.4	67.0	91.3	52.2	83.0	40.0	73.1	29.6	39.1	59.5	74.6	131.9	134.0		
MD-SAN [61]	82.4	96.5	67.4	91.6	52.8	83.6	40.7	73.7	29.8	39.4	59.8	75.0	133.4	135.4		
I^2 OA [64]	82.4	96.6	67.4	91.6	52.8	83.8	40.6	74.0	29.9	39.5	59.8	75.3	133.7	135.6		
CBTrans	82.3	96.5	67.5	91.8	52.8	83.7	40.5	73.5	30.0	39.6	59.6	75.0	135.0	138.6		

TABLE VIII

PERFORMANCE COMPARISON WITH TRANSFORMER BASED ALTERNATIVES, WHICH HAVE THE SAME PARAMETERS, ON MSCOCO VALIDATION SET.

Models	Metrics			
	CIDEr	Score	Optimization	
	B@4	M	C	S
Up-Down Feat.				
Transformer(L2R)	38.9	28.9	127.6	22.6
Transformer(R2L)	36.5	28.9	129.2	22.7
CBTrans	38.0	29.1	129.8	22.8
VinVL Feat.				
Transformer(L2R)	41.0	29.8	134.9	23.6
Transformer(R2L)	37.8	29.6	136.1	23.6
CBTrans	40.0	30.1	137.5	24.2

TABLE X

PERFORMANCE COMPARISON WITH UP-DOWN BASED ALTERNATIVES, WHICH HAVE THE SAME PARAMETERS, ON MSCOCO VALIDATION SET. VINVL FEATURE IS USED HERE.

Models	Metrics			
	CIDEr	Score	Optimization	
	B@4	M	C	S
UpDown(L2R)				
UpDown(L2R)	39.0	29.0	130.6	22.5
UpDown(R2L)				
UpDown(R2L)	36.1	28.7	132.0	22.5
CBLSTM				
CBLSTM	38.4	29.1	133.5	22.9
Removing Bad Endings				
UpDown(R2L)	37.5	28.6	130.8	22.4
CBLSTM	39.1	29.1	132.9	22.8

trick, as shown in the bottom part of Table X.

3) *How does our models perform compared with state-of-the-art models?:* We show the performance comparisons between our models and state-of-the-art models on 'Karpathy' test split in Table I. The performances of the single model and model ensemble are separately reported. The training manners of the Cross-Entropy Loss and CIDEr Score Optimization are also separately reported. The implementation of model ensemble follows the common practice [29], [31], which averaging the word-level output probability distributions of four independently trained instances with different parameter initialization. In general, our CBTrans model exhibits better performance than other models except for X-LAN [3] and RSTNet [16] in BLEU metrics in the single model setting. In the model ensemble setting, our CBTrans model outperforms all other models in all metrics, especially a large margin in CIDEr (about 5%). We think this is partly due to our CBTrans model can simultaneously take advantage of both word-level ensemble and sentence-level ensemble in ensemble setting. In addition, we also report the performance of our ensemble model on the online testing server. Table VII details the performance over official testing images with 5 reference captions (c5) and 40 reference captions (c40). The results clearly show that our CBTrans model shows better performance across

129.8 (22.8) in CIDEr (SPICE) metric. And the advantage is more obvious when using better VinVL feature by improving CIDEr (SPICE) metric from 134.9 (23.6) to 137.5 (24.2).

CBLSTM model also holds this advantage as shown in Table X, e.g., improving the conventional UpDown(L2R) model from 130.6 (22.5) to 133.5 (22.9) in CIDEr (SPICE) metric. However, we find that R2L 'branch' shows an undesirable phenomenon after CIDEr score optimization, i.e., generating some bad endings, e.g.'of a man with a soccer ball on a field'. This undermines the overall model to some extent and causes degradation in BLEU metrics (e.g., from 39.0 to 38.4 in Table X), which focus on n-gram matching. Fortunately, this behavior can be eliminated by using removing bad endings

Cross-Entropy Loss		CIDEr Score Optimization		
Good Cases	Good Cases	Better Feature Effect	Bad Cases	
 <p>Transformer(I2r): a man riding a bike down a street next to a tall building. Transformer(r2l): a group of people riding bikes down a city street. CBTrans: a group of people riding bikes down a city street. CBTrans(VinVL-feat): a group of people riding bikes down a street. GT: a group of bicyclists are riding in the bike lane.</p>	 <p>Transformer(I2r): a man standing on a field with a soccer ball. Transformer(r2l): a group of people playing with a soccer ball on a field. CBTrans: a group of people playing soccer on a field. CBTrans(VinVL-feat): a group of men playing soccer on a field. GT: some men are playing soccer on a field with a blue ball.</p>	 <p>Transformer(I2r): a blue car parked on the grass with a UNK. Transformer(r2l): of an old truck with a UNK on top of it. CBTrans: a blue car parked in the grass with a UNK. CBTrans(VinVL-feat): an old blue car with a surfboard on top of it. GT: an old car with surfboards on the top.</p>	 <p>Transformer(I2r): a man standing on a field with a soccer ball. Transformer(r2l): of a man with a soccer ball on a field. CBTrans: of a man with a soccer ball on a field. CBTrans(VinVL-feat): a man holding a soccer ball on a field. GT: the soccer player is bringing back the ball into play.</p>	 <p>Transformer(I2r): a man standing on a field with a soccer ball.</p>
 <p>Transformer(I2r): a row of motorcycles parked on a street. Transformer(r2l): two motorcycles are parked outside of a building. CBTrans: a row of motorcycles parked in front of a building. CBTrans(VinVL-feat): a row of parked motorcycles sitting on the side of a street. GT: a row of motorcycles parked in front of a building.</p>	 <p>Transformer(I2r): a baseball player is on a field with a ball. Transformer(r2l): on top of a baseball player standing on a field. CBTrans: a baseball player standing on a field with a ball. CBTrans(VinVL-feat): of a baseball player throwing a ball on a field. GT: a baseball player prepares to throw the ball.</p>	 <p>Transformer(I2r): a motorcycle parked on top of a wooden table. Transformer(r2l): of a motorcycle parked next to a shelf. CBTrans: a motorcycle parked on top of a wooden shelf. CBTrans(VinVL-feat): a motorcycle parked in front of a bar of wine bottles. GT: a motorbike sitting in front of a wine display case.</p>	 <p>Transformer(I2r): a man standing on a beach flying a kite. Transformer(r2l): a person is flying a kite on the beach. CBTrans: of a man flying a kite on the beach. CBTrans(VinVL-feat): of a man walking on the beach flying a kite. GT: a man flying a kite over a sandy beach.</p>	

Fig. 4. Examples of captions generated by our CBTrans model, conventional unidirectional Transformer model and human-annotated ground truth. Some bad words are marked in red.

all metrics, e.g., making the absolute improvement over the best competitor RSTNet by 4.1%/4.6% in CIDEr c5/c40. It is noteworthy that we don't list recent vision-language pre-training models [32]–[34] for comparison since it's not fair to directly compare them with non-pretraining-finetuning models.

D. Qualitative Results

We showcase some qualitative results generated by our CBTrans model and conventional unidirectional Transformer model, coupled with human-annotated ground truth sentences (GT) in Fig. 4. On average, CBTrans model can steal from both Transformer(I2r) and Transformer(r2l) models. For example, the CBTrans model absorbs the '*a row of*' of Transformer (I2r) and the '*of a building*' of Transformer (r2l) and generates a caption that is closer to ground truth in the bottom-left example. In the top-left example, CBTrans seems to directly choose the output of Transformer (r2l), which is the better one. We illustrate the effect of using a better feature in the 3rd column, e.g., CBTrans model fed with VinVL feature recognizes '*surfboard*' and '*a bar of wine bottles*'. In the 4th column, we also show a kind of representative bad case of CBTrans model after CIDEr score optimization. This bad endings issue mainly derives from Transformer (r2l) 'flow'. This is probably due to some prepositions (e.g., '*of*') frequently follow '*a*' in the reverse version of ground truth captions. This issue may be alleviated by using trick of removing bad endings or adding BLEU metric to the score function during self-critical training. We also showcase some qualitative results of CBLSTM model in Fig. 5. The first three are good cases

and the last two are bad cases. Basically, CBLSTM model has similar advantage as CBTrans model.

V. CONCLUSION

In this paper, we introduce a compact bidirectional Transformer model for image captioning (CBTrans) that can leverage bidirectional context implicitly and explicitly and the decoder can be executed parallelly. We conduct extensive ablation studies on MSCOCO benchmark and find that the compact architecture, which serves as a regularization for implicitly exploiting bidirectional context, and the sentence-level ensemble play more important roles than the explicit interaction mechanism. We further propose to combine word-level and sentence-level ensemble seamlessly and extend the conventional self-critical training to achieve new state-of-the-art results in comparison with non-vision-language-pretraining models. Finally, we verify the generality of this compact bidirectional architecture by extending it to LSTM backbone. The proposed method is orthogonal to other sophisticated methods for image captioning, including vision-language pretraining, and we leave integrating these methods for better performance as our future work.

REFERENCES

- [1] O. Vinyals, A. Toshev, S. Bengio, and D. Erhan, "Show and tell: A neural image caption generator," in *Proceedings of the IEEE conference on computer vision and pattern recognition*, 2015, pp. 3156–3164.
- [2] X. Yang, K. Tang, H. Zhang, and J. Cai, "Auto-encoding scene graphs for image captioning," in *Proceedings of the IEEE/CVF Conference on Computer Vision and Pattern Recognition*, 2019, pp. 10 685–10 694.

Image_id:151204		<p>Up-Down(l2r): a man riding on the back of an elephant. Up-Down(r2l): a man standing next to a red fire hydrant. CBLSTM: a man riding on the back of an elephant. GT: a person riding an elephant and carrying gas cylinders.</p>
Image_id:15113		<p>Up-Down(l2r): a blue bird sitting on a tree branch. Up-Down(r2l): a colorful bird sitting on a tree branch. CBLSTM: a colorful bird is sitting on a tree branch. GT: a bird that is on a tree limb.</p>
Image_id:345998		<p>Up-Down(l2r): a woman and a child riding on a horse. Up-Down(r2l): a woman and a little girl riding on a horse. CBLSTM: a woman standing next to a girl on a horse. GT: a woman walks beside a horse while a girl rides.</p>
Image_id:143931		<p>Up-Down(l2r): a blue bus with a man standing in front of it. Up-Down(r2l): a sign is painted on the side of a bus. CBLSTM: a blue bus with a flag on the side of it. GT: a large bus with a political ad on the side of it.</p>
Image_id:318671		<p>Up-Down(l2r): a horse pulling a trolley on a city street. Up-Down(r2l): of people in a horse drawn carriage on a street. CBLSTM: of a white horse pulling a carriage on a street. GT: people riding on a horse trolley in the street.</p>

Fig. 5. Examples of captions generated by our CBLSTM model, conventional unidirectional Up-Down model and human-annotated ground truth.

- [3] Y. Pan, T. Yao, Y. Li, and T. Mei, “X-linear attention networks for image captioning,” in *Proceedings of the IEEE/CVF Conference on Computer Vision and Pattern Recognition*, 2020, pp. 10971–10980.
- [4] Y. Zhou, Y. Zhang, Z. Hu, and M. Wang, “Semi-autoregressive transformer for image captioning,” in *Proceedings of the IEEE/CVF International Conference on Computer Vision (ICCV) Workshops*, October 2021, pp. 3139–3143.
- [5] Y. Huang, J. Chen, W. Ouyang, W. Wan, and Y. Xue, “Image captioning with end-to-end attribute detection and subsequent attributes prediction,” *IEEE Transactions on Image Processing*, vol. 29, pp. 4013–4026, 2020.
- [6] H. Liu, S. Zhang, K. Lin, J. Wen, J. Li, and X. Hu, “Vocabulary-wide credit assignment for training image captioning models,” *IEEE Transactions on Image Processing*, vol. 30, pp. 2450–2460, 2021.
- [7] X. Yang, H. Zhang, and J. Cai, “Auto-encoding and distilling scene graphs for image captioning,” *IEEE Transactions on Pattern Analysis and Machine Intelligence*, 2020.
- [8] Y. Wang, J. Xu, and Y. Sun, “End-to-end transformer based model for image captioning,” in *Proceedings of the AAAI Conference on Artificial Intelligence*, vol. 36, no. 3, 2022, pp. 2585–2594.
- [9] N. Wang, J. Xie, J. Wu, M. Jia, and L. Li, “Controllable image captioning via prompting,” in *Proceedings of the AAAI Conference on Artificial Intelligence*, vol. 37, no. 2, 2023, pp. 2617–2625.
- [10] N. Wang, J. Xie, H. Luo, Q. Cheng, J. Wu, M. Jia, and L. Li, “Efficient image captioning for edge devices,” in *Proceedings of the AAAI Conference on Artificial Intelligence*, vol. 37, no. 2, 2023, pp. 2608–2616.
- [11] A.-A. Liu, Y. Zhai, N. Xu, H. Tian, W. Nie, and Y. Zhang, “Event-aware retrospective learning for knowledge-based image captioning,” *IEEE Transactions on Multimedia*, vol. 26, pp. 4898–4911, 2024.
- [12] P. Song, Y. Zhou, X. Yang, D. Liu, Z. Hu, D. Wang, and M. Wang, “Efficiently gluing pre-trained language and vision models for image captioning,” *ACM Transactions on Intelligent Systems and Technology*, vol. 15, no. 6, pp. 1–16, 2024.
- [13] J. Zhang, K. Zhang, Y. Xie, and Z. Wang, “Deep reciprocal learning for image captioning,” *IEEE Transactions on Circuits and Systems for Video Technology*, 2025.
- [14] I. Sutskever, O. Vinyals, and Q. V. Le, “Sequence to sequence learning with neural networks,” in *Advances in neural information processing systems*, 2014, pp. 3104–3112.
- [15] A. Vaswani, N. Shazeer, N. Parmar, J. Uszkoreit, L. Jones, A. N. Gomez, Ł. Kaiser, and I. Polosukhin, “Attention is all you need,” in *Advances in neural information processing systems*, 2017, pp. 5998–6008.
- [16] X. Zhang, X. Sun, Y. Luo, J. Ji, Y. Zhou, Y. Wu, F. Huang, and R. Ji, “Rstnet: Captioning with adaptive attention on visual and non-visual words,” in *Proceedings of the IEEE/CVF Conference on Computer Vision and Pattern Recognition*, 2021, pp. 15465–15474.
- [17] X. Yang, H. Zhang, and J. Cai, “Deconfounded image captioning: A causal retrospect,” *IEEE Transactions on Pattern Analysis and Machine Intelligence*, 2021.
- [18] F. Sammani and M. Elsayed, “Look and modify: Modification networks for image captioning,” *arXiv preprint arXiv:1909.03169*, 2019.
- [19] F. Sammani and L. Melas-Kyriazi, “Show, edit and tell: A framework for editing image captions,” in *Proceedings of the IEEE/CVF Conference on Computer Vision and Pattern Recognition*, 2020, pp. 4808–4816.
- [20] L. Wang, Z. Bai, Y. Zhang, and H. Lu, “Show, recall, and tell: Image captioning with recall mechanism,” in *Proceedings of the AAAI Conference on Artificial Intelligence*, vol. 34, no. 07, 2020, pp. 12176–12183.
- [21] Z. Song, X. Zhou, Z. Mao, and J. Tan, “Image captioning with context-aware auxiliary guidance,” in *Proceedings of the AAAI Conference on Artificial Intelligence*, vol. 35, no. 3, 2021, pp. 2584–2592.
- [22] Z. Zhang, Z. Qi, C. Yuan, Y. Shan, B. Li, Y. Deng, and W. Hu, “Open-book video captioning with retrieve-copy-generate network,” in *Proceedings of the IEEE/CVF Conference on Computer Vision and Pattern Recognition*, 2021, pp. 9837–9846.
- [23] K. Xu, J. Ba, R. Kiros, K. Cho, A. Courville, R. Salakhudinov, R. Zemel, and Y. Bengio, “Show, attend and tell: Neural image caption generation with visual attention,” in *International conference on machine learning*. PMLR, 2015, pp. 2048–2057.
- [24] H. Jiang, I. Misra, M. Rohrbach, E. Learned-Miller, and X. Chen, “In defense of grid features for visual question answering,” in *Proceedings of the IEEE/CVF Conference on Computer Vision and Pattern Recognition*, 2020, pp. 10267–10276.
- [25] P. Anderson, X. He, C. Buehler, D. Teney, M. Johnson, S. Gould, and L. Zhang, “Bottom-up and top-down attention for image captioning and visual question answering,” in *Proceedings of the IEEE conference on computer vision and pattern recognition*, 2018, pp. 6077–6086.
- [26] T. Yao, Y. Pan, Y. Li, and T. Mei, “Exploring visual relationship for image captioning,” in *Proceedings of the European conference on computer vision (ECCV)*, 2018, pp. 684–699.
- [27] J. Gu, G. Wang, J. Cai, and T. Chen, “An empirical study of language cnn for image captioning,” in *Proceedings of the IEEE International Conference on Computer Vision*, 2017, pp. 1222–1231.
- [28] M. Cornia, M. Stefanini, L. Baraldi, and R. Cucchiara, “Meshed-memory transformer for image captioning,” in *Proceedings of the IEEE/CVF Conference on Computer Vision and Pattern Recognition*, 2020, pp. 10578–10587.
- [29] L. Huang, W. Wang, J. Chen, and X.-Y. Wei, “Attention on attention for image captioning,” in *Proceedings of the IEEE/CVF International Conference on Computer Vision*, 2019, pp. 4634–4643.
- [30] Y. Zhou, M. Wang, D. Liu, Z. Hu, and H. Zhang, “More grounded image captioning by distilling image-text matching model,” in *Proceedings of the IEEE/CVF Conference on Computer Vision and Pattern Recognition*, 2020, pp. 4777–4786.
- [31] S. J. Rennie, E. Marcheret, Y. Mroueh, J. Ross, and V. Goel, “Self-critical sequence training for image captioning,” in *Proceedings of the IEEE conference on computer vision and pattern recognition*, 2017, pp. 7008–7024.
- [32] L. Zhou, H. Palangi, L. Zhang, H. Hu, J. Corso, and J. Gao, “Unified vision-language pre-training for image captioning and vqa,” in *Proceedings of the AAAI Conference on Artificial Intelligence*, vol. 34, no. 07, 2020, pp. 13041–13049.
- [33] X. Li, X. Yin, C. Li, P. Zhang, X. Hu, L. Zhang, L. Wang, H. Hu, L. Dong, F. Wei *et al.*, “Oscar: Object-semantics aligned pre-training for vision-language tasks,” in *European Conference on Computer Vision*. Springer, 2020, pp. 121–137.
- [34] P. Zhang, X. Li, X. Hu, J. Yang, L. Zhang, L. Wang, Y. Choi, and J. Gao, “Vinvl: Revisiting visual representations in vision-language models,” in *Proceedings of the IEEE/CVF Conference on Computer Vision and Pattern Recognition*, 2021, pp. 5579–5588.
- [35] C. Wang, H. Yang, C. Bartz, and C. Meinel, “Image captioning with deep bidirectional lstms,” in *Proceedings of the 24th ACM international conference on Multimedia*, 2016, pp. 988–997.
- [36] R. Caruana, “Multitask learning,” *Machine learning*, vol. 28, no. 1, pp. 41–75, 1997.

[37] W. Zhao, B. Wang, J. Ye, M. Yang, Z. Zhao, R. Luo, and Y. Qiao, “A multi-task learning approach for image captioning,” in *IJCAI*, 2018, pp. 1205–1211.

[38] A. Deshpande, J. Aneja, L. Wang, A. G. Schwing, and D. Forsyth, “Fast, diverse and accurate image captioning guided by part-of-speech,” in *Proceedings of the IEEE/CVF Conference on Computer Vision and Pattern Recognition*, 2019, pp. 10 695–10 704.

[39] B. Wang, L. Ma, W. Zhang, W. Jiang, J. Wang, and W. Liu, “Controllable video captioning with pos sequence guidance based on gated fusion network,” in *Proceedings of the IEEE/CVF International Conference on Computer Vision*, 2019, pp. 2641–2650.

[40] J. Hou, X. Wu, W. Zhao, J. Luo, and Y. Jia, “Joint syntax representation learning and visual cue translation for video captioning,” in *Proceedings of the IEEE/CVF International Conference on Computer Vision*, 2019, pp. 8918–8927.

[41] D. Elliott, S. Frank, and E. Hasler, “Multilingual image description with neural sequence models,” *arXiv preprint arXiv:1510.04709*, 2015.

[42] X. Li, C. Xu, X. Wang, W. Lan, Z. Jia, G. Yang, and J. Xu, “Coco-en for cross-lingual image tagging, captioning, and retrieval,” *IEEE Transactions on Multimedia*, vol. 21, no. 9, pp. 2347–2360, 2019.

[43] X. Wang, J. Wu, J. Chen, L. Li, Y.-F. Wang, and W. Y. Wang, “Vatex: A large-scale, high-quality multilingual dataset for video-and-language research,” in *Proceedings of the IEEE/CVF International Conference on Computer Vision*, 2019, pp. 4581–4591.

[44] Z. Song, Z. Hu, Y. Zhou, Y. Zhao, R. Hong, and M. Wang, “Embedded heterogeneous attention transformer for cross-lingual image captioning,” *IEEE Transactions on Multimedia*, vol. 26, pp. 9008–9020, 2024.

[45] D. Bahdanau, K. Cho, and Y. Bengio, “Neural machine translation by jointly learning to align and translate,” *arXiv preprint arXiv:1409.0473*, 2014.

[46] Z. Zhang, S. Wu, S. Liu, M. Li, M. Zhou, and T. Xu, “Regularizing neural machine translation by target-bidirectional agreement,” in *Proceedings of the AAAI Conference on Artificial Intelligence*, vol. 33, no. 01, 2019, pp. 443–450.

[47] Y.-C. Chen, Z. Gan, Y. Cheng, J. Liu, and J. Liu, “Distilling knowledge learned in bert for text generation,” in *Proceedings of the 58th Annual Meeting of the Association for Computational Linguistics*, 2020, pp. 7893–7905.

[48] J. Devlin, M.-W. Chang, K. Lee, and K. Toutanova, “Bert: Pre-training of deep bidirectional transformers for language understanding,” *arXiv preprint arXiv:1810.04805*, 2018.

[49] X. Zhang, J. Su, Y. Qin, Y. Liu, R. Ji, and H. Wang, “Asynchronous bidirectional decoding for neural machine translation,” in *Proceedings of the AAAI Conference on Artificial Intelligence*, vol. 32, no. 1, 2018.

[50] L. Zhou, J. Zhang, and C. Zong, “Synchronous bidirectional neural machine translation,” *Transactions of the Association for Computational Linguistics*, vol. 7, pp. 91–105, 2019.

[51] S. Hochreiter and J. Schmidhuber, “Long short-term memory,” *Neural computation*, vol. 9, no. 8, pp. 1735–1780, 1997.

[52] S. Ren, K. He, R. Girshick, and J. Sun, “Faster r-cnn: Towards real-time object detection with region proposal networks,” *Advances in neural information processing systems*, vol. 28, pp. 91–99, 2015.

[53] K. He, X. Zhang, S. Ren, and J. Sun, “Deep residual learning for image recognition,” in *Proceedings of the IEEE conference on computer vision and pattern recognition*, 2016, pp. 770–778.

[54] J. L. Ba, J. R. Kiros, and G. E. Hinton, “Layer normalization,” *arXiv preprint arXiv:1607.06450*, 2016.

[55] R. Vedantam, C. Lawrence Zitnick, and D. Parikh, “Cider: Consensus-based image description evaluation,” in *Proceedings of the IEEE conference on computer vision and pattern recognition*, 2015, pp. 4566–4575.

[56] R. Luo, “A better variant of self-critical sequence training,” *arXiv preprint arXiv:2003.09971*, 2020.

[57] T. Yao, Y. Pan, Y. Li, Z. Qiu, and T. Mei, “Boosting image captioning with attributes,” in *Proceedings of the IEEE international conference on computer vision*, 2017, pp. 4894–4902.

[58] W. Jiang, L. Ma, Y.-G. Jiang, W. Liu, and T. Zhang, “Recurrent fusion network for image captioning,” in *Proceedings of the European Conference on Computer Vision (ECCV)*, 2018, pp. 499–515.

[59] Y. Qin, J. Du, Y. Zhang, and H. Lu, “Look back and predict forward in image captioning,” in *Proceedings of the IEEE/CVF Conference on Computer Vision and Pattern Recognition*, 2019, pp. 8367–8375.

[60] Z. Li, J. Wei, F. Huang, and H. Ma, “Modeling graph-structured contexts for image captioning,” *Image and Vision Computing*, vol. 129, p. 104591, 2023.

[61] J. Ji, X. Huang, X. Sun, Y. Zhou, G. Luo, L. Cao, J. Liu, L. Shao, and R. Ji, “Multi-branch distance-sensitive self-attention network for image captioning,” *IEEE Transactions on Multimedia*, vol. 25, pp. 3962–3974, 2023.

[62] J. Yan, Y. Xie, Y. Guo, Y. Wei, and X. Luan, “Exploring better image captioning with grid features,” *Complex & Intelligent Systems*, vol. 10, no. 3, pp. 3541–3556, 2024.

[63] C. Cai, K.-H. Yap, and S. Wang, “Toward attribute-controlled fashion image captioning,” *ACM Transactions on Multimedia Computing, Communications and Applications*, vol. 20, no. 9, pp. 1–18, 2025.

[64] X. Zhang, A. Jia, J. Ji, L. Qu, and Q. Ye, “Intra-and inter-head orthogonal attention for image captioning,” *IEEE Transactions on Image Processing*, vol. 34, pp. 594–607, 2025.

[65] T. Yao, Y. Pan, Y. Li, and T. Mei, “Hierarchy parsing for image captioning,” in *Proceedings of the IEEE/CVF International Conference on Computer Vision*, 2019, pp. 2621–2629.

[66] X. Chen, H. Fang, T.-Y. Lin, R. Vedantam, S. Gupta, P. Dollár, and C. L. Zitnick, “Microsoft coco captions: Data collection and evaluation server,” *arXiv preprint arXiv:1504.00325*, 2015.

[67] A. Karpathy and L. Fei-Fei, “Deep visual-semantic alignments for generating image descriptions,” in *Proceedings of the IEEE conference on computer vision and pattern recognition*, 2015, pp. 3128–3137.

[68] K. Papineni, S. Roukos, T. Ward, and W.-J. Zhu, “Bleu: a method for automatic evaluation of machine translation,” in *Proceedings of the 40th annual meeting of the Association for Computational Linguistics*, 2002, pp. 311–318.

[69] S. Banerjee and A. Lavie, “Meteor: An automatic metric for mt evaluation with improved correlation with human judgments,” in *Proceedings of the acl workshop on intrinsic and extrinsic evaluation measures for machine translation and/or summarization*, 2005, pp. 65–72.

[70] C.-Y. Lin, “Rouge: A package for automatic evaluation of summaries,” in *Text summarization branches out*, 2004, pp. 74–81.

[71] P. Anderson, B. Fernando, M. Johnson, and S. Gould, “Spice: Semantic propositional image caption evaluation,” in *European conference on computer vision*. Springer, 2016, pp. 382–398.

[72] D. P. Kingma and J. Ba, “Adam: A method for stochastic optimization,” *arXiv preprint arXiv:1412.6980*, 2014.

[73] G. Li, L. Zhu, P. Liu, and Y. Yang, “Entangled transformer for image captioning,” in *Proceedings of the IEEE/CVF International Conference on Computer Vision*, 2019, pp. 8928–8937.

[74] J. Ji, Y. Luo, X. Sun, F. Chen, G. Luo, Y. Wu, Y. Gao, and R. Ji, “Improving image captioning by leveraging intra-and inter-layer global representation in transformer network,” in *Proceedings of the AAAI Conference on Artificial Intelligence*, vol. 35, no. 2, 2021, pp. 1655–1663.